

4-1999

Performance of sinusoidally deformed hydrophone line arrays

Deanna M. Caveny

Donald R. Del Balzo

James H. Leclere

George E. Ioup
University of New Orleans

Follow this and additional works at: https://scholarworks.uno.edu/phys_facpubs



Part of the [Physics Commons](#)

Recommended Citation

J. Acoust. Soc. Am. 105, 2203 (1999)

This Article is brought to you for free and open access by the Department of Physics at ScholarWorks@UNO. It has been accepted for inclusion in Physics Faculty Publications by an authorized administrator of ScholarWorks@UNO. For more information, please contact scholarworks@uno.edu.

Performance of sinusoidally deformed hydrophone line arrays

Deanna M. Caveny,^{a)} Donald R. Del Balzo, and James H. Leclere
Naval Research Laboratory, Stennis Space Center, Mississippi 39529

George E. loup
Department of Physics, University of New Orleans, New Orleans, Louisiana 70148

(Received 31 January 1997; revised 2 April 1998; accepted 14 December 1998)

It is well known that array deformations can distort beam patterns and introduce bearing errors if the beamformer assumes linearity. It is also known that deformed arrays can resolve left–right ambiguities, provided the shape is known. In this work, these two effects are studied for undamped and damped sinusoidally deformed arrays with small deformation amplitudes in the horizontal (x, y) plane only. By use of fixed arc-length separations along the array, the hydrophone (x, y) coordinates are determined numerically and the error in assuming equal x spacing is summarized for a sample array. Array-response patterns are analyzed for two conditions: (1) when the deformed array shape is assumed linear and (2) when the deformed array shape is known exactly. Degradations resulting from assuming linearity and the ability to resolve left–right ambiguities are discussed in terms of reduced gain, degraded angular resolution, and bearing errors. Shape-unknown signal-gain degradation ranges to 7 dB at broadside, but is less than 1 dB near endfire. For the shape-known case, signal gain for the true peak is greater than signal gain for the ambiguous peak by up to 9 dB for sources at broadside and to just over 2.5 dB for arrivals near endfire. © 1999 Acoustical Society of America. [S0001-4966(99)06103-2]

PACS numbers: 43.30.Wi, 43.30.Bp [SAC-B]

INTRODUCTION

Hinich and Rule,¹ Hodgkiss,² Bouvet,³ Ginzkey,⁴ and Butler⁵ have shown that deformations from a straight-line shape in the horizontal plane of towed arrays can produce significant distortions in array-response patterns and errors in bearing estimation if the beamformer assumes linearity. Hinich and Rule¹ use approximate undamped and damped sinusoidal shapes and report the case of $3\frac{1}{2}$ half-cycles of the sinusoid. For the damped case, deformation increases with distance from the towing platform. Hodgkiss² employs a single circular arc shape and discusses errors in passive ranging and bearing estimation. Bouvet³ develops a model for large random array variations using fixed sensor separations (nonelastic array) with application to a circular arc. Bouvet³ also gives a helpful brief review of related literature. Ginzkey⁴ studies the effects of small two-dimensional random position errors. Butler⁵ uses a sinusoidal deformation model which assumes equal x spacing of the hydrophones.

More recent work has discussed nonacoustic and acoustic methods to estimate array shapes, without emphasis on performance implications. One nonacoustic method involves direct hydrodynamic modeling based on single-point measurements either on the tow ship or on the cable itself with motion propagated along the array.^{6–9} Another is based on distributed measurements from nonacoustic sensors along the array (e.g., depth gauges and compasses).^{10,11} Generally, these techniques rely on solving the Paidoussis equation and/or interpolating between known points with polynomials or splines. The acoustic approaches involve a variety of

signal-processing techniques using acoustic signals received at the hydrophones in two general categories—(a) from near-field controlled sources, and (b) from far-field noncontrolled sources of opportunity. The first approach usually involves arrival-time measurements from explosive sources^{12,13} and the second often exploits relative phase information by working in the frequency domain.^{14–16}

The issue of practical determination of array shapes is addressed well by the references above and others, and is not discussed further. The work reported here examines the impact (either good or bad) of array deformations (both known and unknown) in terms of beamformer performance and left–right ambiguity resolution.

This work examines the performance of towed arrays with small, horizontal deformations, primarily caused by unplanned variations in the tow-ship trajectory. The array-shape model is also capable of treating larger deformations, which could result from planned tow-ship maneuvers. The physical basis for the shape model derives from a harmonically driven damped oscillator, with small steering corrections of the towing platform providing the driving force. The attachment (or tow) point between the steel tow cable and the neutrally buoyant horizontal array is the origin for this model, and it is approximated to be a fixed node. A short vibration isolation module (VIM) is inserted between the tow point and the hydrophone array. The model produces an array shape based on the number of cycles (whole or fractional), the amplitude, and a damping factor. A drogue is assumed to be attached to the aft end of the array; thus, the damping in this model decreases the deformation as one moves away from the tow point, in contrast to the model of Hinich and Rule.¹

This study is based on acoustic field modeling and

^{a)}Present address: Department of Mathematics, College of Charleston, Charleston, SC 29424.

beamforming using computer software¹⁷ that generates cross-spectral matrices for arbitrary hydrophone locations in specified noise fields. The results presented here use conventional beamforming with infinitely high signal-to-noise ratio on horizontal arrays with sinusoidal deformations. The fixed arc-length method of defining array shapes is described, along with a comparison of beamformer performance between known and unknown shapes. Finally, a discussion of the impact of array deformation on gain and bearing ambiguity resolution is given.

I. DETERMINATION OF HYDROPHONE X-Y LOCATIONS

To approximate a sinusoidal shape, Hinich and Rule¹ use straight-line segments between hydrophones. To calculate the locations of hydrophones for the sinusoidal models without approximation, however, it is necessary to fix the hydrophone spacing along the array curve and determine the x and y (horizontal plane) coordinates. This models an elastic array with varying sensor separations, overcoming the limitation discussed by Bouvet.³ The vertical variable z is assumed constant for this study. The method for determining the coordinates involves the numerical evaluation of the arc-length integral. In the limit of small sinusoidal amplitudes, the hydrophones can be assumed to have equally spaced x locations, greatly simplifying the calculation. For the present work, only the arc-length integral method is used, and neither the assumption of equally spaced x locations⁵ nor the assumption of straight-line segments between hydrophones¹ is employed.

The natural dimensions for scaling position variables and other length measures for deformed, equally spaced hydrophone arrays are the array element spacing, d , and the design wavelength, λ , which is assumed to be $2d$. The array is simulated to contain a forward VIM with arc-length of $6d$, followed by 128 hydrophones, and terminated by a drogue for stability. The first hydrophone is at an arc-length of $d/2$ from the point where the VIM connects to the hydrophone array. Each succeeding sensor is separated by an arc-length d along the curve from the previous one.

The problem is stated as follows. Assume that the towed array takes the shape of an undamped or damped sinusoid. Given a specific number of cycles, the undamped amplitude, and the amount of damping, determine the (x, y) coordinate location of each hydrophone. An equation for the array shape can be written as

$$y(x) = Ae^{-ax} \sin(\pi x/w), \quad (1)$$

where the undamped amplitude, A , and the amount of damping, a , are specified. The third parameter, w , although fixed by the number of cycles, is not known initially. It is to be determined before the coordinates are calculated.

Consider an undamped sine curve of p cycles. Let L denote the total array length, which is $(N+5.5)d$ if there are N hydrophones and the VIM is $6d$ in length. Then, the arc-length between two adjacent nodes for an undamped array is $L/2p$. The arc-length integral is given by

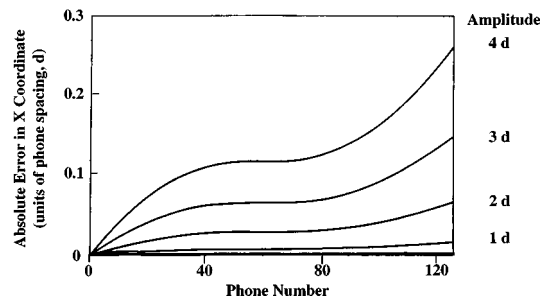


FIG. 1. The absolute error in the x -coordinate vs hydrophone number of a 128-element array resulting from the assumption of equal spacing d along the x axis. The array shape is an undamped $1/2$ -cycle sine, with deformation amplitudes from $0.5d$ to $4.0d$.

$$I_U(A, L) = \int_0^u [1 + A^2 q^2 \cos^2 qx]^{1/2} dx, \quad (2)$$

where $q = p/w$ and u and w are to be determined. Various approaches may be used; for example, one could choose $u = L/2p$ and $w = u$ and use numerical integration to refine these values until a specified tolerance between the calculated and known arc-lengths is reached.

In the damped case, the equal spacing of the zero-crossings (or nodes) is preserved, but the array length between any two adjacent nodes is no longer a constant. The arc-length integral is given by

$$I_D(A, L, a) = \int_0^u [1 + A^2 e^{-2ax} (a \sin qx - q \cos qx)^2]^{1/2} dx. \quad (3)$$

In this case, the upper limit of the arc-length integral (i.e., the unknown value u) is chosen to be the x -coordinate of the last hydrophone. Then, the known arc-length is the total array length. Initially, u is taken to be L , and $w = u/2p$. The arc-length expression (3) can be evaluated and u adjusted, with $w = u/2p$, until the integral is close enough to L .

The x -coordinate of each hydrophone is found in a similar fashion, except that w is now determined and u gives the hydrophone x -coordinate. The integration arc-length is initially from the tow point to the first hydrophone, or generally from the last known hydrophone location to the adjacent unknown location. The corresponding y -coordinates are easily calculated from Eq. (1).

If instead one assumes that the x -coordinates are equally spaced with spacing d , the numerical integration could be avoided. For sine curves with small amplitudes, this assumption introduces only small errors. But the magnitude of the error grows with increasing hydrophone number and increasing array-deformation amplitudes. The assumption of this equal spacing always shifts the x -coordinates in a positive direction, making the array appear longer than it actually is, and the accumulated error increases more rapidly when the tangent line to the sine curve is steeper. Figure 1 illustrates the absolute value of the error in the x -coordinate of each hydrophone as a function of hydrophone number for arrays with $1/2$ -cycle distortion of various deformation amplitudes. The cumulative effect of the equal spacing assumption is evident, especially for the larger array amplitudes. The de-

TABLE I. Array geometries.

Cases	σ/λ	A	a	Shape
a	0.0	0.0	0	Linear
b	0.3	2.13	0	Half cycle
c	0.3	1.47	0	Full cycle
d	0.3	0.87	0	1 1/2 cycle
e	0.2	2.13	0.0069	Half cycle
f	0.1	2.13	0.0200	Half cycle

viations of the true x positions from equal x spacing do not become larger than $0.1d$ ($\lambda/20$) until the deformation of the array is greater than $2d$ for a 1/2-cycle sine array of 128 hydrophones.

II. EXAMPLES OF DEFORMED ARRAY BEAMFORMING

Hodgkiss² investigates plane-wave beamforming for various source locations and circular arc array shapes. His results are given as array-response plots when beamforming with both the actual circular arc hydrophone locations and assumed linear locations. He does not consider left-right ambiguity resolution and his array-response patterns go over only 180 deg. Similar studies are conducted here for arrays having undamped and damped sinusoidal geometries, with the addition of an examination of left-right ambiguity resolution and the calculation of performance curves.

Six array geometries are considered in this study: (a) a linear array for reference; (b) an undamped 1/2-cycle deformation with amplitude of 2.13 hydrophone spacings; (c) an undamped full-cycle deformation with amplitude of 1.47 hydrophone spacings; (d) an undamped 1 1/2-cycle deformation with amplitude of 0.87 hydrophone spacings; (e) a damped 1/2-cycle deformation with maximum amplitude of 1.55 hydrophone spacings ($A=2.13d$ and $a=0.0069$); and (f) a more highly damped 1/2-cycle deformation with maximum amplitude of 0.95 hydrophone spacings ($A=2.13d$ and $a=0.020$). These amplitude and damping factor values were chosen to produce a value for the undamped cases of 0.3 in the array shape statistic, σ/λ , with σ the rms shape distortion as measured from a best-fitting straight line, and values of 0.2 and 0.1, respectively, for the damped cases. The cases are summarized in Table I.

The source azimuths considered in this section are 90 (broadside), 45, and 10 deg from endfire, all at the design frequency and all in the horizontal plane. Calculations for out-of-plane arrivals (10 deg from the horizontal) were made and shown to be consistent with the in-plane results (to within 0.003 dB) and therefore are excluded from the study. Figure 2 illustrates the beamformed array-response patterns (with equal weighting on each hydrophone and no background noise) for a linear array over the full 360 deg azimuthal sector. The upper plot shows the 90 deg (broadside) source azimuth result. The middle and lower plots show the 45 and 10 deg source results, respectively. Note the standard results of beam broadening away from broadside and the occurrence of grating lobes as the signal approaches endfire. Figures 3–5 contain array-response patterns for sinusoidally deformed arrays assuming that beamforming is implemented

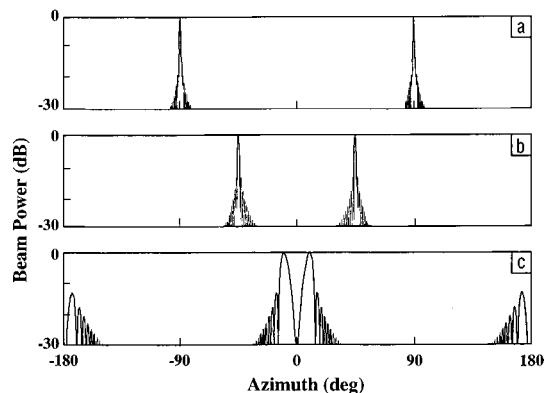


FIG. 2. Linear array responses for sources at (a) 90 deg, (b) 45 deg, and (c) 10 deg from endfire.

with both (1) the incorrect assumption that the array geometry is linear, and (2) the actual hydrophone locations known. The responses shown in Fig. 2 are included so that the deformed array responses can be compared. Beam powers for all figures are referenced to 0 dB for the linear array-response maximum at a given source direction. None of the responses below -30 dB is plotted.

Figure 3 shows the response of the undamped 1/2-cycle sine array with $\sigma/\lambda=0.3$ to sources at 90 deg in (a) and (b), 45 deg in (c) and (d), and 10 deg in (e) and (f). In Fig. 3(a), (c), and (e), the array shape is assumed known and the actual element locations are used in the beamforming. Since the distorted array has almost the same total aperture as the linear array, the forward (true) peak is almost identical to that for the linear response. The ambiguous (false) peak, however, does not have the same phase delays for the deformed array as the forward peak does, so it is significantly changed. It has less signal gain, is broader, and is broken up into several local maxima for the sources at 90 and 45 deg. While the ambiguous peak at -10 deg (corresponding to a source at 10 deg) is somewhat reduced and broadened, it is not broken up in the same way as the others. This is due to two factors: (a) the array has less resolution (wider beams) near endfire than at broadside, and (b) a plane wave arriving in a direction close to endfire sees a smaller array deformation than one arriving at broadside. If, as is generally the case, the

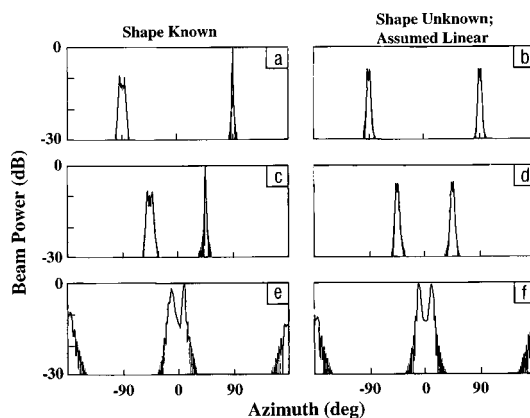


FIG. 3. Undamped 1/2-cycle deformed-array response. Amplitude of deformation is $2.13d$ and σ/λ is 0.3. Source is at 90 deg for (a) and (b), at 45 deg for (c) and (d), and at 10 deg for (e) and (f).

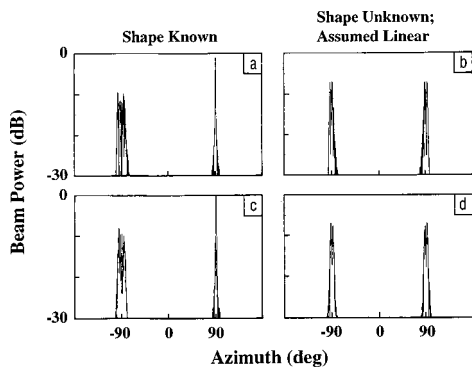


FIG. 4. Undamped full-cycle, (a) and (b), and 1 1/2-cycle, (c) and (d), deformed-array responses for a source at 90 deg. Deformation amplitude for full cycle is $1.47d$, and for 1 1/2 cycles is $0.87d$. σ/λ for both cases is 0.3.

array shape is unknown and beamforming is done assuming the shape to be linear, the responses of Fig. 3(b), (d), and (f) result. The signal gain is reduced, especially at 90 and 45 deg, where the response peaks are also split. At 10 deg, the reduction in gain is small and the main peak shape is close to that of the linear response, again because the deformation looks smaller and the beams are wider near endfire.

For the remaining array shapes, only the array response to a broadside arrival is shown. The second and third undamped examples are in Fig. 4, while the damped cases are illustrated in Fig. 5. For the undamped arrays, $\sigma/\lambda=0.3$, the same value as the 1/2-cycle undamped array of Fig. 3. The general behavior of the responses of the full-cycle array, Fig. 4(a) and (b), and the 1 1/2-cycle array, Fig. 4(c) and (d), is similar to that of the broadside responses of the 1/2-cycle array. The ambiguous peak in the shape-known responses and both the true and ambiguous peaks in the shape-unknown responses exhibit fine structure. This is because the deformed-array shapes themselves have structure. In effect, the deformed array is composed of several nearly straight subsections, each of which has its own natural direction. Thus, the incident plane wave is resolved into multiple directions.

Since the damped arrays of Fig. 5 (both 1/2 cycle) have smaller values of σ/λ (0.2 and 0.1) than the undamped cases, the shape-unknown responses are closer to the linear array

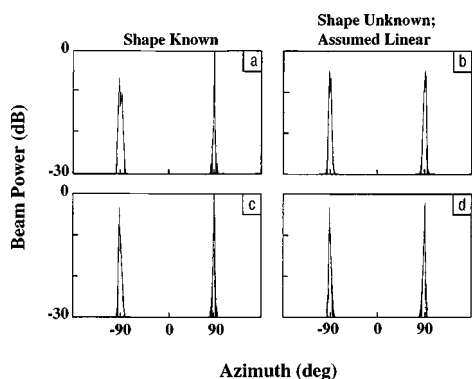


FIG. 5. Damped 1/2-cycle deformed-array response for a source at 90 deg. (a) and (b) are for a shape determined by $A=2.13d$, $a=0.0069$, and $\sigma/\lambda=0.2$, while (c) and (d) are for an array with $A=2.13d$, $a=0.020$, and $\sigma/\lambda=0.1$.

response at broadside than the undamped responses of Figs. 3 and 4. Thus, for the unknown-shape case, the drogue seems beneficial to performance because it increases damping, which in turn decreases physical deformations, leading to reduced beamformer phase-delay errors when linearity is assumed. This produces greater signal power through the beamformer.

The irregular nature of the broken peaks in Figs. 3 through 5 leads to instabilities in such performance measures as peak height, bearing, and beamwidth because of the difficulty in defining these quantities. The splitting of the true peak when the beamforming is done assuming a linear array leads to bearing errors resulting from choosing the largest subpeak. This suggests that for arrays which have a large enough aperture and enough deformation to produce this splitting, it may be better to fit a smooth analytic shape in order to estimate signal gain, source direction, and beamwidth.

Note that the shape-unknown responses are all symmetric about 0 deg in Figs. 3–5. This is because differences in the field as sensed by a distorted array correspond to phase shifts (from the phases of a linear array) that are equal and opposite to the phase errors in the steering vectors that result from assuming that the distorted array is straight. To understand this result, consider the phases at the hydrophones for arrival directions of plus and minus θ . For the deformed arrays, arrivals from $+\theta$ will have, at each hydrophone, a shifted phase Δ_+ from the phase value at a straight line array, and arrivals from $-\theta$ will have a different shifted phase Δ_- . These phase shifts will be incorporated into the cross-spectral matrix for both shape-known and shape-unknown beamforming. For shape-unknown beamforming, the steering vectors correspond to a linear array. Thus, the phase errors in these steering vectors are opposite to the phase differences in the cross-spectral matrix mentioned above, and therefore the plus and minus arrival directions have the same (incorrect) array response.

III. PERFORMANCE DEGRADATION FOR DEFORMED ARRAYS

Hodgkiss² quantifies degradations in the beamforming process, with the incorrect assumption of linearity, for known circular arc shapes as a function of the amount of bow. This section contains a systematic study of performance degradation for sinusoidally deformed arrays when the shape is unknown, in terms of three measures: (1) signal gain, (2) beamwidth broadening, and (3) bearing shifts. The signal-to-noise ratio is infinite and the signal degradation is considered for σ/λ in the range of 0.0 to 0.3.

Figure 6 addresses the first issue, signal gain, by showing the power loss in the true peaks in the shape-unknown case, relative to the linear-array peak power, plotted versus σ/λ , for various array damped and undamped shapes (half cycles, full cycles, 1 1/2 cycles) and for various source azimuths. The azimuths selected are 10, 30, 45, 60, and 90 deg for the 1/2-cycle cases, and 10 and 90 deg for the others. For the damped array, σ/λ may be varied by changing either the amplitude (controlled primarily by tow-ship trajectory varia-

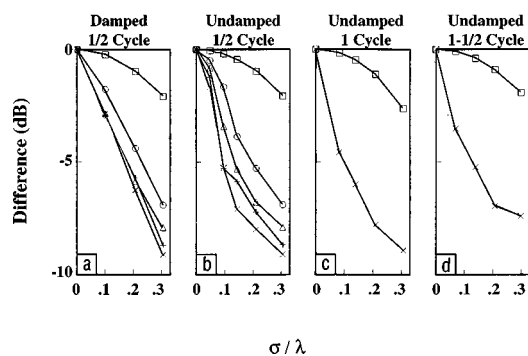


FIG. 6. Performance curves of peak-height degradation for deformed arrays assumed to be linear. Loss in array-signal gain of deformed arrays is given as the power loss in the source peaks, in dB, relative to the corresponding peaks for a linear array, versus σ/λ for sources at 10 (\square), 30 (\circ), 45 (\triangle), 60 ($+$), and 90 deg (\times).

tions) or the damping factor (controlled primarily by the drogue characteristics). This performance evaluation is conducted by varying the damping factor.

For all cases, the degradation is greatest for broadside arrivals (6–7 dB when $\sigma/\lambda=0.3$), decreasing, in general, as the source arrival angle approaches endfire (about 0.5 dB when $\sigma/\lambda=0.3$ for the 10 deg source). The small exceptions, as before, are due to the irregular qualities of the degraded peaks. As expected, the degradation becomes worse with increasing array deformations (i.e., greater σ/λ) for all shapes. For a given source direction, the degradations are similar for all combinations considered, except for the results corresponding to the 90 and 60 deg source directions. For these arrival angles, among the cases examined, only the 1/2-cycle undamped and the full-cycle performance for sources at broadside track fairly closely. The performance at $\sigma/\lambda=0.3$, however, is identical for all arrival angles for the damped and undamped 1/2-cycle cases because the two array shapes are identical since the damped array has $\sigma/\lambda=0.3$ when the damping is exactly zero.

One practical application of performance summaries, such as those shown in Fig. 6, is to determine, as a function of σ/λ , if the array-element locations need be known or if the beamforming process can assume a linear array. As an example, given a full-cycle, damped or undamped, deformed array and broadside arrivals, if no more than a 5-dB loss in signal gain is acceptable, then array-element locations are needed when $\sigma/\lambda>0.2$. If no more than a 3-dB loss is tolerable, then the approximate upper limit for assuming linearity is $\sigma/\lambda=0.13$. These findings are consistent with the general loss in signal gain for Gaussian errors in element locations given by Steinberg¹⁸ in his Fig. 6 and the accompanying discussion. Note that these σ/λ limits are a function of array shape, and that for broadside arrivals they are higher for 1 1/2-cycle arrays and lower for damped and undamped 1/2-cycle arrays.

Second, distorted arrays can produce beam broadening. One can consider the true-peak beamwidth for shape-unknown beamforming as a measure of performance degradation by comparing it to the beamwidth for the true peak in the corresponding linear-array response. Although not quantified here, significant true-peak broadening can be observed

in the shape-unknown response patterns of Figs. 3 through 5. Performance curves for true-peak broadening as a result of assuming linearity serve as a measure, which, along with the loss in array-signal gain, can be used to determine the largest acceptable value of σ/λ for shape-unknown beamforming.

Third, distorted arrays can produce bearing errors. For small values of σ/λ , incorrectly assuming a linear array may result in only small losses in signal gain and beam resolution. In these instances, one may choose to accept this degradation. As Hinich and Rule¹ and Hodgkiss² point out, however, there can still be a bearing error of 1 to 2 deg. This bearing error arises from the splitting of the true peak into two or more subpeaks, the largest of which is not centered with respect to the peak spread. For the deformed-array responses shown in this paper, only damped 1/2-cycle responses are included for deformations with σ/λ less than 0.3. In Fig. 5(b), $\sigma/\lambda=0.1$ and the peak is already asymmetrical, although not highly broken. For $\sigma/\lambda=0.2$, the response shown in Fig. 5(d) is split into two parts with a minimum between them at the correct source bearing. The broadside $\sigma/\lambda=0.3$ peaks, shown for various array shapes in Figs. 3(b) and 4(b) and (d), exhibit behavior ranging from a simple splitting into two parts to a highly broken and irregular shape. Thus, it is understandable that even relatively small array deformations lead to bearing errors as large as approximately half the true-peak beamwidth in shape-unknown beamforming. Hinich¹⁹ and Bouvet³ (and references cited therein) discuss techniques for estimating the correct bearing.

IV. LEFT–RIGHT AMBIGUITY RESOLUTION FOR DEFORMED ARRAYS WITH KNOWN SHAPE

The standard technique to resolve left–right ambiguities on nominally straight towed arrays is first to record the two possible true bearings toward a source, second to make a course change, and third to note the new possible true bearings. A consistency check will give the correct bearing. Unfortunately, during a course change, uncorrected array deformations can be so severe that loss in beamformer signal gain can cause a loss in source detection (against noise). After the turn is completed and the tow-ship trajectory has stabilized, there is still a residual time required for the array to straighten and stabilize. For some applications, these time delays are unsatisfactory. A process which could allow continuous monitoring of the true source bearing without loss in detection time is desirable.

Both Hinich and Rule,¹ and Hodgkiss² discuss advantages of a deformed array over a linear array to discriminate true from ambiguous peaks. This section examines two approaches for continuous left–right ambiguity resolution for sinusoidally deformed arrays when the shape is known. The first involves the power difference, and the second involves the beam width ratio between the true and ambiguous peaks. All of the results are discussed in terms of the amount of array distortion, as defined by the σ/λ measure, with infinite signal-to-noise ratio. Figure 7 illustrates the power loss in the “false,” or ambiguous, peak. This loss is plotted vs σ/λ for various array damped and undamped shapes (half cycles, full cycles, 1 1/2 cycles) and for various source azimuths. The

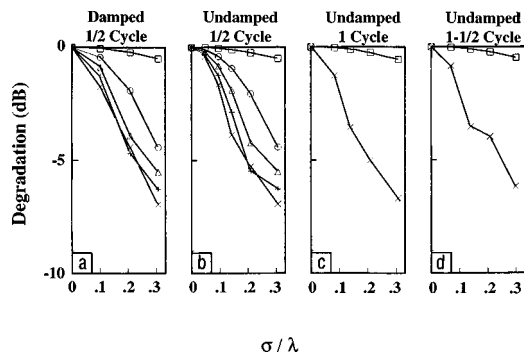


FIG. 7. Performance curves for peak-height difference in left-right ambiguity resolution of deformed arrays with known element locations. Amount by which left (ambiguous) peak is down from right (true) peak is given in dB versus σ/λ for sources at 10 (\square), 30 (\circ), 45 (\triangle), 60 ($+$), and 90 deg (\times).

azimuths selected are 10, 30, 45, 60, and 90 deg for the 1/2-cycle cases and 10 and 90 deg for the others.

In Fig. 7(a), the 1/2-cycle damped array performance is given for left-right ambiguity resolution in terms of true peak minus ambiguous peak power difference in dB versus σ/λ . In general, for this and all cases in Fig. 7, the ability to discriminate an ambiguous peak from a true peak by power difference is greatest for sources at broadside, and decreases to be least for sources close to endfire. This trend is expected because the left-right phase difference is smaller at endfire. Deviations from this observation are slight in Fig. 7, and occur because of the instabilities in the broken ambiguous peak maxima discussed earlier.

The first observation from Fig. 7 is based on a comparison of 7(a) and (b) where the array is distorted into the same general shape (i.e., 1/2 cycle) but with and without damping. For a given σ/λ , the undamped array almost always has greater power differences, and is therefore a better left-right source discriminator, for source azimuths away from endfire. Thus, damping is generally deleterious to performance when attempting to resolve left-right ambiguities by true peak-ambiguous peak power differences. This is in contrast to the previous conclusion that damping is beneficial when considering beam power (signal gain) on a distorted array assumed linear. There is a tradeoff between the two countering effects which can be evaluated for a given scenario.

In Fig. 7(b), (c), and (d), the left-right ambiguity resolution performance for the undamped 1/2-cycle, full cycle, and 1 1/2-cycle arrays can be compared. At broadside, for a given σ/λ , the undamped half and full cycle arrays are better (i.e., have greater power difference) at resolving left-right ambiguity than a 1 1/2-cycle array. An examination of Figs. 3(a) and 4(a) and (c), however, shows that for $\sigma/\lambda=0.3$, this advantage in ambiguity resolution is due mainly to two thin spikes in a highly broken 1 1/2-cycle ambiguous peak. If an average or curve-fit peak is used instead of the tallest sub-peak to measure ambiguity resolution, this distinction in the difference performance measure is not expected to be as large.

The other approach for left-right ambiguity resolution concerns beam broadening. Beamforming with the known hydrophone locations gives true peaks which correspond

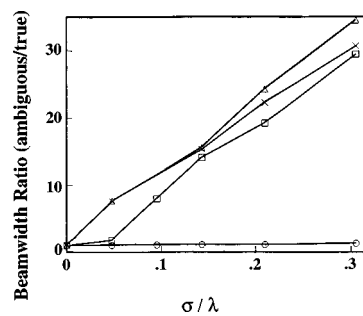


FIG. 8. Left-right ambiguity beamwidth resolution. The beamwidth ratio, defined as the false-peak 3-dB width over the true-peak 3-dB width, for deformed arrays beamformed with array-element locations known, versus σ/λ . Results are given for a 1/2-cycle array (\square), a full-cycle array (\triangle), and a 1 1/2-cycle array (\times) for a broadside source and also for a 1/2-cycle array (\circ) with a source at 10 deg.

closely, in terms of 3-dB beamwidth, to the true peaks which a linear array would produce for the small deformations considered here. For the ambiguous peaks, on the other hand, the broadening is large and the ratio of the 3-dB beamwidth of the ambiguous peak to that of the true peak may be taken as another measure of left-right ambiguity resolution. In Fig. 8, this ratio is given, as a function of σ/λ , for all three undamped cases with broadside arrivals and for the undamped 1/2-cycle case with a 10 deg arrival. For broadside incidence, the ratio of the beamwidths for the ambiguous peak to the true peak increases rapidly with increasing σ/λ to a value of 30 to 35 at $\sigma/\lambda=0.3$ for all three shapes. It is possible that, at small deformations, this ratio may be a better discriminator for left-right ambiguity resolution than the difference in signal gain for sources at broadside in some applications. For the 1/2-cycle deformation and a source at 10 deg, however, the beamwidth ratio is almost constant at 1, versus σ/λ , and so would not serve as a useful discriminant. The 3-dB beamwidths of the broken ambiguous peaks have been determined as accurately as possible without recourse to curve fitting and may be subject to small errors.

It should be noted that the shape-unknown beamwidths in the previous section are smaller for all these examples than the beamwidths of the ambiguous peaks in the associated shape-known responses. Therefore, in this limited range of calculations for shape-known beamforming, the ratios shown in Fig. 8 are larger than would be found for shape-unknown beamforming. This result is not surprising, since the phase errors for the ambiguous peaks for shape-known beamforming are, in a sense, twice those of shape-unknown beamforming.

V. CONCLUSIONS

This paper reports results of array performance as affected by known and unknown distortions in array shape. Using a simple but accurate model of hydrophone positions, which produces an array with equal arc-lengths between elements, various array configurations were constructed. These included undamped and damped 1/2-cycle sinusoidal configurations and also undamped full-cycle and 1 1/2-cycle configurations.

In shape-known beamforming, the ability to discriminate true peaks from ambiguous peaks increases as array deformation increases. Differences in array-signal gain for these two peaks range up to 9 dB for $\sigma/\lambda=0.3$ when the source is at broadside. For arrivals near endfire, however, the largest difference is only about 2.5 dB. In shape-unknown beamforming, the degradation in array-signal gain ranges up to 7 dB at broadside, but remains less than 1 dB near endfire. The results can be used to determine if shape estimation is required.

Beamwidths of the ambiguous peaks were compared to beamwidths of the true peaks in shape-known beamforming. The ratio of these beamwidths increases rapidly with σ/λ , reaching a value of 30–35 at $\sigma/\lambda=0.3$ for the full-cycle array with the source at broadside. The true-peak broadening for shape-unknown beamforming is also significant, but less than that of the ambiguous peak. Near endfire, the broadening is negligible for both types of beamforming for the domain of σ/λ considered.

Straightforward measures of array signal-gain degradation and beamwidths are difficult to apply due to the broken nature of the peaks with the resolution capability of 128 hydrophones ($64\text{-}\lambda$ array). This problem also leads to errors in bearing estimation.

Regarding the question of the utility of drogues to stabilize towed arrays, there is an apparent dichotomy. Drogues reduce array horizontal deformations, and this improves signal gain for the shape-unknown case with linearity assumed. However, array straightening hinders left–right signal discrimination. Thus, use of drogues may depend on the specific objectives and scenarios.

ACKNOWLEDGMENTS

The authors wish to acknowledge the financial support of the Naval Undersea Warfare Center and of the Office of Naval Research. The authors are extremely grateful to Art Collier of the Canadian Defense Research Establishment Atlantic for supplying BEAMSTATPAK, a powerful and general computer-software package for modeling acoustic signal and noise fields and for beamforming. Helpful discussions with Don Murphy and Jeff Beckleheimer of NRL are also acknowledged.

- ¹M. J. Hinich and W. Rule, "Bearing estimation using a towed array," *J. Acoust. Soc. Am.* **58**, 1023–1029 (1975).
- ²W. S. Hodgkiss, "The effects of array shape perturbation on beamforming and passive ranging," *IEEE J. Ocean Eng.* **8**, 120–130 (1983).
- ³M. Bouvet, "Beamforming of a distorted line array in the presence of uncertainties on the sensor positions," *J. Acoust. Soc. Am.* **81**, 1833–1840 (1987).
- ⁴L. Ginzkey, "Influence of sensor position errors on spatial signal processing algorithms," in *Proceedings of NATO ASI on Adaptive Methods in Underwater Acoustics*, Luneburg, Germany, 30 July–10 August 1985, edited by H. Urban (Reidel, Dordrecht, 1985), pp. 477–482.
- ⁵D. Butler, "Beamforming with a distorted towed array," in *Proceedings of NATO ASI on Adaptive Methods in Underwater Acoustics*, Luneburg, Germany, 30 July–10 August 1985, edited by H. Urban (Reidel, Dordrecht, 1985), pp. 469–475.
- ⁶C. Lee, "A modeling study on steady-state and transverse dynamic motion of a towed array system," *IEEE J. Ocean Eng.* **3**, 14–21 (1978).
- ⁷J. Ketchman, "Vibration induced in towed linear underwater array cables," *IEEE J. Ocean Eng.* **6**, 77–86 (1981).
- ⁸D. R. Del Balzo, "Observations of towed array vertical stability and horizontal shape during SACLANTCEN Cruise LRG 1/89," SACLANTCEN SR-220, La Spezia, Italy (1993).
- ⁹C. S. van Aartsen, "The Response Model," in *Proceedings of Low Frequency Active Acoustics Conference*, La Spezia, Italy, SACLANT Undersea Research Center (1993).
- ¹⁰D. A. Gray, B. D. O. Anderson, and R. R. Bitmead, "Towed array shape estimation using Kalman filters—theoretical models," *IEEE J. Ocean Eng.* **18**, 543–556 (1993).
- ¹¹B. E. Howard and J. M. Syck, "Calculation of the shape of a towed underwater acoustic array," *IEEE J. Ocean Eng.* **17**, 193–203 (1993).
- ¹²L. J. Rosenblum and D. R. Del Balzo, "A constructive algorithm for determining array shape with application to Fredex," Naval Research Lab, Washington, DC, NRL Repert 8531 (1979).
- ¹³E. C. Ballegooijen, G. W. M. Mierlo, C. van Schooneveld, P. P. M. van der Zalm, A. T. Parsons, and N. H. Field, "Measurement of towed array position, shape, and attitude," *IEEE J. Ocean Eng.* **14**, 375–383 (1989).
- ¹⁴B. G. Quinn, R. F. Barrett, P. J. Kootsookos, and S. J. Searle, "The estimation of the shape of an array using a hidden Markov model," *IEEE J. Ocean Eng.* **18**, 557–564 (1993).
- ¹⁵B. G. Ferguson, "Remedying the effects of array shape distortion on the spatial filtering of acoustic data from a line array of hydrophones," *IEEE J. Ocean Eng.* **18**, 565–571 (1993).
- ¹⁶D. E. Wahl, "Towed array shape estimation using frequency-wavenumber data," *IEEE J. Ocean Eng.* **18**, 582–590 (1993).
- ¹⁷J. H. Leclere, D. R. Del Balzo, H. A. Chandler, R. R. Slater, and G. E. Ioup, "A brief introduction to BEAMSTATPAK with sample calculations of array performance on multiple line systems," NORDA Tech Note 49, Naval Res. Lab., Stennis Space Center, MS (1991).
- ¹⁸B. D. Steinberg, *Principles of Aperture and Array System Design* (Wiley, New York, 1976).
- ¹⁹M. J. Hinich, "Bearing estimation using a perturbed linear array," *J. Acoust. Soc. Am.* **61**, 1540–1544 (1977).